Paper Number 156

ANALYSIS OF MAIN ROTOR NOISE REDUCTION DUE TO NOVEL PLANFORM DESIGN – THE BLUE EDGE™ BLADE

M. Gervais
marc.gervais@eurocopter.com

V. Gareton
vincent.gareton@eurocopter.com

EUROCOPTER
Aéroport International Marseille-Provence
13725 Marignane, FRANCE

ABSTRACT

This paper presents a detailed analysis of the acoustic measurements performed on an aircraft equipped with Blue Edge™ blades. These blades incorporate a novel double-swept planform designed to reduce Blade-Vortex Interaction (BVI) noise in descending flight. The analysis presented herein demonstrates through full scale near-field and far-field noise measurements that the new blade shape efficiently reduces BVI noise throughout the flight envelope of the aircraft. Using various metrics to assess the Blue Edge™ blades compared to standard straight blades, the paper shows that the level and directivity of BVI noise is greatly altered due to the forward/backward blade sweep. Results show that the baseline rotor propagates strong BVI noise toward the front and retreating side of the rotor, and that the new blades offer the best gains for these directivities. Also, it is shown that significant BVI noise is generated on the baseline rotor's retreating side and propagates behind the aircraft, and that the Blue Edge™ rotor is also successful at reducing these interactions. Finally, preliminary noise footprints are shown to highlight the potential of these blades in terms of operational noise reduction.

INTRODUCTION

The noise generated by rotorcraft and received by observers in the far-field reflects the complexity of the aerodynamic environment in which these aircraft operate. Many sources are involved (main and tail rotors, engine, transmission), and each of these sources vary differently in level, frequency content, and directivity according to the flight condition. For many years, it has been recognised that the one of the most penalising noise source is Blade-Vortex Interactions (BVI), which generates loud, impulsive, and strongly directive noise mainly during descending flight conditions. BVI results from the interaction of the vortices created by the main rotor blades with its own blades.

A typical BVI occurs when a blade tip vortex shed in the second quadrant is impacted by a following blade in the first quadrant (see Figure 1). This type of advancing side BVI is quite penalising because of the high Mach numbers experienced by the blade on the advancing side. The noise typically propagates efficiently toward the front of the rotor, either toward the advancing or retreating sides. Interactions can also occur on the retreating side, where tip vortices shed in the third quadrant are impacted by a blade in the fourth quadrant. These interactions propagate toward the rear of the rotor. The following figure schematically illustrates BVI events on the advancing and retreating sides for a three-bladed rotor (only one tip vortex is shown for simplicity).

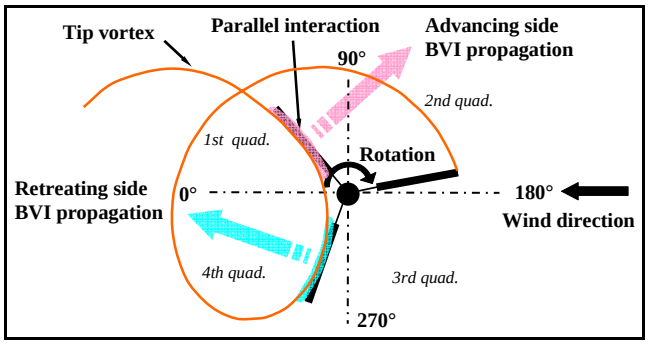

Figure 1 : Typical parallel Blade-Vortex Interactions on the advancing and retreating blade sides

The main parameters governing BVI noise are:
- the strength and size of the vortices generated by the blade, which is mainly driven by the loading distribution and the speed at the blade tip ;
- the blade/vortex 'miss-distance' which is the distance in the vertical plane between the blade and the vortex and which is mainly governed by the induced velocity through the rotor ;
- the geometry of interaction in the rotor disk plane, or how the vortices are positioned with respect to the blade at the time of interaction, and which is a function rotor speed and advance ratio.

Design solutions aimed at reducing BVI noise therefore target a modification of these three parameters, either through passive technologies (blade planform, tip shape, twist, airfoil distribution, etc), through active technologies (higher harmonic control, individual blade control), or through a modification of the aircraft trim (noise abatement procedures). This paper focuses on a passive noise reduction mechanism based on a modification of the blade planform which impacts mostly the geometry of the interactions.

The geometry of the interaction in the rotor disk plane, as illustrated in Figure 1, dictates how the acoustic waves accumulate in the far field at a given observer location. These so-called 'phasing effects' drastically affect the level and frequency characteristic of the noise perceived by the observer (Ref. [1]). When the acoustic pressure disturbances generated by the BVI at each blade spanwise section are received by an observer substantially at the same time, the total acoustic pressure tends to be high and

impulsive in nature. Contrarily, when these pressure disturbances are spread in time, the total acoustic pressure can be significantly reduced because of an out-of-phase addition (or even cancellation) of the acoustic pressure from each spanwise section.

Interactions that are termed 'parallel' (for which the entire blade span impacts a vortex simultaneously) cause all the acoustic pressure disturbances to be received at the same time by an observer in a direction perpendicular to the blade leading edge. These therefore tend to be very penalising. Advancing side parallel interactions are particularly penalising because of the high blade speed. Note that BVI is mainly a leading edge dominated event since most of the rapid aerodynamic loading changes created as the vortex passes over the blade occur near the leading edge.

The Blue Edge™ concept aims to reduce the strength of BVI noise in the most penalising conditions/directions by avoiding strong parallel interaction simultaneously over the entire blade span (see Figure 2). Parallel interactions still occur on certain portion of the blade, but the large forward/backward sweep prevents the acoustic pressures from accumulating over the entire span. Also, the backward sweep on the outboard part of the blade causes a parallel interaction which exhibits a main propagation directivity toward the side of the aircraft (almost perpendicular to the flight direction). This directivity is beneficial because the component of the Mach number in the direction of the observer in this case is lower than for an interaction propagating toward the centreline, and therefore the Doppler amplification factor is reduced. Finally, the gradual but pronounced blade taper causes a smoother blade loading distribution which reduces the strength of the tip vortex.

The Blue Edge™ Programme

This double swept blade design concept had initially been studied within the ERATO project (study of an Acoustical and Technological Rotor Optimisation, Ref. [2]) which was launched by ONERA, DLR, and Eurocopter.

Following the conclusion of the ERATO project, Eurocopter signed at the end of 2000 a research agreement with ONERA that was supported by the DGAC in order to develop a full-scale blade for flight testing. The details of this programme have previously been presented in Ref. [3]. The four-phase programme started from the lessons learnt of ERATO, and continued through detailed blade design, manufacturing, and finally full-scale testing on an EC155 demonstrator aircraft. The following figure shows the planform evolution from ERATO to Blue Edge™.

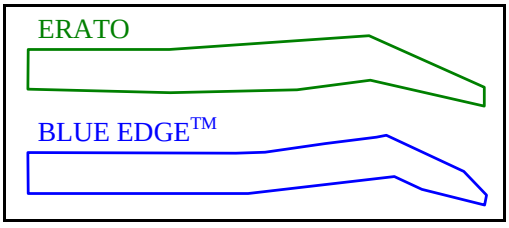

Figure 2 : Comparison of the blade planform between ERATO and Blue Edge™

The flight test campaign, which began in 2007, was performed throughout the entire flight envelope of the aircraft and covered evaluations of the performance, static and dynamic loads, vibrations, handling qualities, and acoustics of the new blade. Typically, these flight test evaluations were performed as comparative studies with the reference EC155 rotor, with flights performed successively with the same aircraft equipped with the two different sets of blades. By the end of the programme, more than 75 flight hours had been performed with the rotor fitted with Blue Edge™ blades. This paper focuses on the acoustic evaluations that were performed in 2007 and 2008 as part of this research programme.

FLIGHT TEST DESCRIPTION

As mentioned previously, the Blue Edge™ blades are designed specifically to reduce BVI noise in the approach phase. To demonstrate the efficiency of noise reduction, two different flight test measurements were performed on a full-scale demonstrator (EC155) with a standard rotor equipped with straight blades and a Blue Edge™ rotor equipped with double swept blades (see Figure 3). The baseline rotor is comprised of straight blades with a parabolic tip.

Figure 3 : EC155 equipped with Blue Edge™ blades during noise measurements.

A first noise test campaign aimed at measuring and comparing the noise characteristics of the two different rotors over the whole flight envelope (including flyover, approach, and climb) with a set of near-field microphones attached to the outside the aircraft. This test was aimed at quickly validating that the concept tested on a four-bladed rotor in the wind tunnel scaled adequately to a real aircraft with a five-bladed rotor.

Once this risk reduction test was validated, a second flight test campaign was conducted, covering several flight conditions with a matrix of seven ground microphones to assess the direct comparison of the baseline and Blue Edge™ rotors.

Near-field microphone flight test

The first flight campaign was performed on the whole flight envelope in order to confirm the capability of the Blue Edge™ rotor to reduce BVI noise in comparison with the reference main rotor. The near-field microphones were attached to the outside of the airframe as shown on Figure 4, with three microphones installed on the advancing blade side and two additional microphones attached to the horizontal tail. Nose cones in front of the microphones were used to reduce the aerodynamic noise resulting from the advancing speed. Aerodynamic noise was also reduced thanks to an installation on swivelling weathervanes.

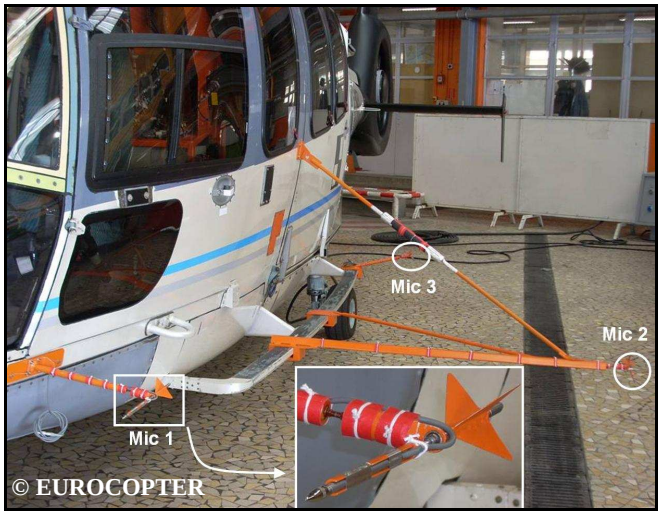

Figure 4 : Near-field microphone installation.

The main interest of such microphone set-up is its low-cost, the possibility to quickly cover the entire flight envelope, and also the ability to test manoeuvring phases. On the other hand, such measurements are quite limited in terms of directivity characteristics: the reduced numbers of microphone do not allow a precise ground noise footprint characterisation.

The flyover and descent flight test matrix that was performed for both rotors for this test campaign is shown below.

Table 1. Test matrix for in-flight microphone campaign

	True Air Speed (kt)						
Rate of Descent	50	60	80	95	115	130	145
0 ft/mn		x	x	x	x	x	x
-250 ft/mn	x	x	x	x	x		
-500 ft/mn	x	x	x	x			
-750 ft/mn	x	x	x	x			
-850 ft/mn		x	x				
-1000 ft/mn	x	x	x	x			
-1250 ft/mn		x	x	x			
-1500 ft/mn		x	x	x			

Ground microphone flight test

The system used to record on-ground sound pressure level is composed of several stations connected via Wi-Fi to a central control station. This measurement instrumentation was previously introduced in detail in Ref. [4]. The measurement stations allow real-time monitoring of all channels installed on the field, and the results are compatible with standard noise certification standards (see for example Refs. [5] and [6]). Synchronized GPS antennae on each station allow time to be strictly monitored and are linked to the aircraft and meteorological station time base.

The microphones used for these ground measurements were standard certification-type pressure-field microphones set at 1.2m. Two seven-microphone transversal arrays were installed on the airfield and the direction of flight was chosen based on the predominant wind direction. For example, when the wind was mainly blowing from the north or south the seven microphones located on the east-west flight track were used. The microphones were located at the following lateral distances: ±300m, ±150m, ±75m, and 0m.

The flyover and descending flight test matrix for this campaign is presented in Table 2 (climb conditions were also performed but are not addressed herein). This matrix was designed to cover the most interesting flight conditions based on the results of the in-flight microphone campaign. All flights were measured both with the standard and the Blue Edge™ main rotor to allow close comparisons.

Table 2. Test matrix for ground microphone campaign

	True Air Speed (kt)						
Glideslope (deg)	50	60	70	80	95	130	145
0						x	x
-2		x	x				
-4	x	x	x	x			
-6	x	x	x	x	x		
-8	x	x	x	x			
-10		x					

RESULTS

Near-field microphones results

Ref. [3] introduced results of the near-field acoustic flight envelope characterisation in the form of an A-weighted contour plot showing the difference between the baseline rotor and the Blue Edge™ rotor. In this paper, each flight envelope plot is shown separately in order to highlight the distinctive features of the two rotors.

The approach flight envelope of the EC155 equipped with the baseline rotor is presented on Figure 5. This figure shows the near-field A-weighted sound pressure level as a function of true airspeed (X-axis) and rate-of-descent (Y-axis). The levels plotted represent microphone #2 on the advancing blade side (see Figure 4), and exhibit a strong BVI noise region for low speeds (between 55 and 85 knots) and moderate glideslope -3 to -9° (i.e. rates-of-descent between -400 to -900 ft/min). This region corresponding to high BVI noise is typical of most rotorcraft. This impulsive noise 'hotspot' is penalising because standard glideslopes and airspeeds used in operational flight procedures usually fall within this high noise region and noise abatement procedures used to avoid this region require steep descent angles, often combined with strong decelerations.

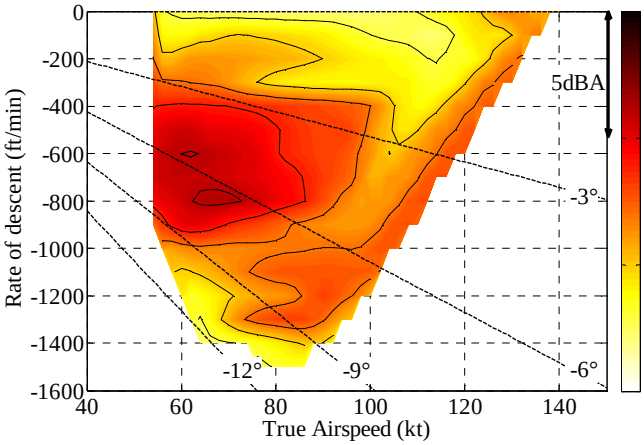

Figure 5 : Near-field A-weighted sound pressure level for reference rotor (contours are 2dBA apart).

Figure 6 presents the same approach flight envelope for the EC155 equipped with Blue Edge™ blades. The high noise level region due to BVI on Figure 5 has been completely eliminated due to the double-swept blades.

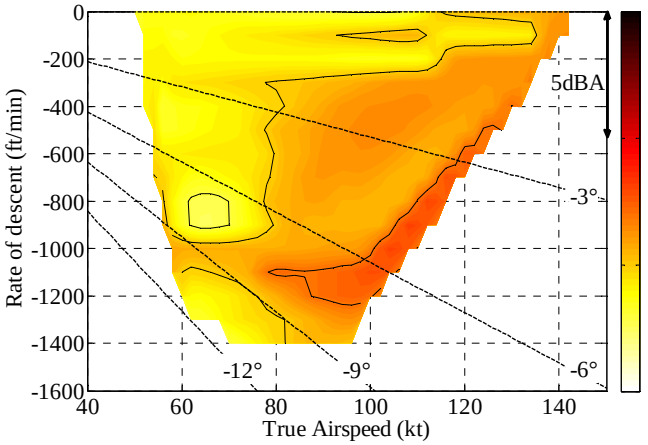

Figure 6 : Near-field A-weighted sound pressure level for Blue Edge™ rotor (contours are 2dBA apart).

In the course of the data processing and analysis, various metrics were used to highlight the presence or absence of BVI noise. These included the standard certification metrics (such as tone-corrected perceived noise level, PNLT), but also dedicated BVI noise metrics. For example, flight envelope graphs such as Figures 5 and 6 were plotted in terms of BVISPL (for which the signal is filtered to show only the 6th through the 40th harmonic of the main rotor). However, the BVISPL plots showed the same trends as the A-weighted plots shown above. The kurtosis of the signal was also used in order to attempt to better characterise the typical impulsivity of BVI noise, and the impact of the Blue Edge™ blades on this impulsivity. The kurtosis (fourth standardized moment of a signal) is a measure of the "peakedness" of a signal or how much this signal exhibits strong/quick variations around a mean value (Ref. [7]). As such, the kurtosis can be used to quantify the amount of BVI present in the near-field microphone pressure level.

Figure 7 presents the difference between the kurtosis of near-field microphone #2 with Blue Edge™ and with the baseline rotor as a function of true airspeed and rate-of-descent. Around the region where BVI is prevalent (low speed approach at -400 to -900 ft/min) for the baseline rotor a strong reduction of kurtosis occurs for Blue Edge™ rotor.

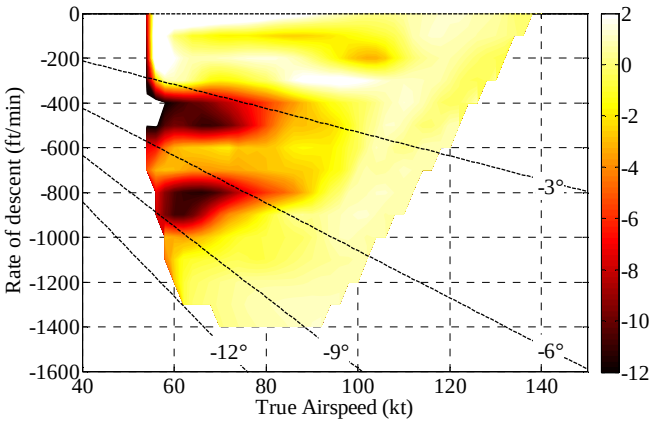

Figure 7 : Difference between near-field kurtosis for the two rotors (negative values where reference rotor has higher kurtosis).

Figures 5 and 6, and Ref. [1], highlight the 60 knots, -8° glideslope approach as the condition which shows the maximum reduction of A-weighted sound pressure level. Figure 7 above shows that the kurtosis also points to this flight condition. However, the preceding figure also shows significant kurtosis reduction for flight conditions at -400 to -500 ft/min between 50 and 70 knots (the 50 knot cases are not shown on the graph because they are at the limit of the interpolation range used to plot the graph). Note that on Figure 7, the two distinct regions of strong kurtosis reduction which are apparent at -450 ft/min and -850 ft/min most probably form a single region covering this whole descent range, the discontinuity between the two regions being due to insufficient data points in that region. The following figure focuses on the pressure time-history of a 55 knots, -4° glideslope approach in order to assess the capability of the kurtosis to properly identify BVI noise in this flight condition.

On Figure 8 the acoustic pressure time-history measured by the near-field microphone #2 is presented for the baseline and Blue Edge™ rotors. The time axis of the figure has been set to fit two rotations of the 5-bladed main rotor. The strong negative peaks of the baseline signal characterize the temporal representation of interaction of a vortex with a blade.

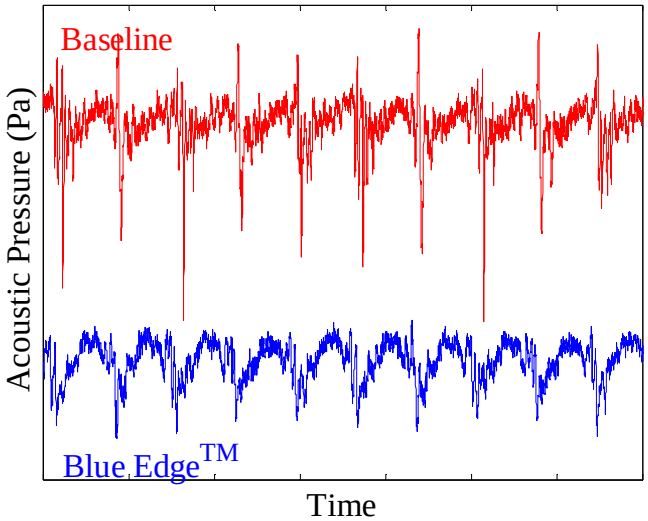

Figure 8 : Acoustic pressure time-history for standard and Blue Edge™ blades for a 55 kt, -4° glideslope approach (pressure scales are identical).

On the previous figure the Blue Edge™ BVI pressure peaks are still present but much less important than the standard rotor. This sample result shows that the kurtosis is indeed able to correctly identify and highlight BVI noise, whereas in this case the A-weighted sound pressure level was insufficient. This highlights the importance of the choice of metrics for representing rotorcraft noise sources. In this specific case, the usual metrics (dB, dBA, PNLT, BVISPL) do not properly qualify the signal and thus underestimate the gains brought by the Blue Edge™ blades in terms of annoyance.

This first in-flight microphones campaign demonstrated the ability of the Blue Edge™ blades to reduce BVI events on a large region of the flight envelope. This successful noise test validated the Blue Edge™ concept on a full scale demonstrator and led to the second phase of the noise test

campaign which aimed at quantifying the expected noise reductions on ground microphones.

Ground microphone flight test

Near-field microphones flight test were conducted with a reduced number of microphones all positioned close to the aircraft structure and mostly on the advancing side of the rotorcraft. Using this setup, it is indeed difficult to estimate the gains on the ground as well as the directivity patterns of BVI noise propagation.

To overcome this issue flight tests were conducted with Blue Edge™ and baseline rotors on an array of seven ground microphones. This second set of test aimed at allowing a direct comparison of the two rotors, quantifying the expected gain of the Blue Edge™ rotor compared to the baseline rotor, and evaluating the directivity characteristics of the new rotor in the far-field.

In order to highlight the difference between the two rotors, this part of the article focuses on a single flight condition (60 knots, -8° glideslope approach) where the best noise reductions in terms of A-weighted sound pressure level were measured. However the explanations for noise reduction and directivity characteristics are applicable to other approach flight conditions where BVI occurs.

Figure 9 presents the effective perceived noise level (EPNL, see Ref. [5]) as a function of the lateral distance for the 60 knots, -8° glideslope approach. For each rotor, the curves represent the average of all runs that were performed at that condition.

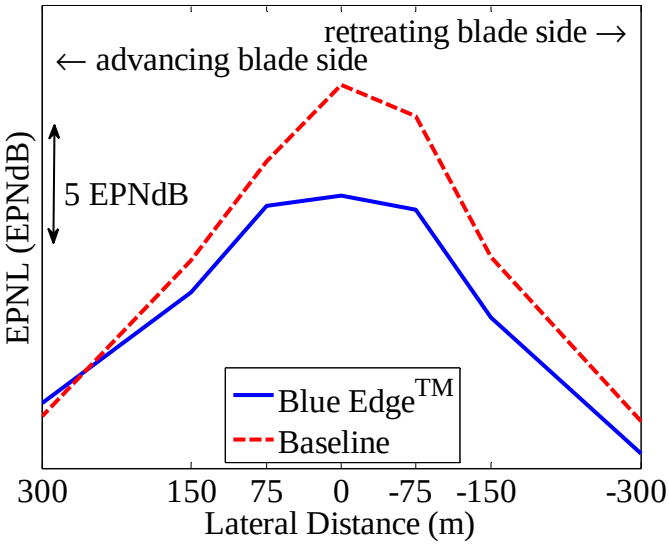

Figure 9 : EPNL as a function of lateral distance for baseline and Blue Edge™ rotors.

Figure 9 shows that the baseline rotor noise levels are significantly higher than the Blue Edge™ rotor results for most microphone positions. It is interesting to note that the most important gains are experienced on the centreline and retreating blade side, contrary to what could be expected from advancing side parallel BVI reduction (see Figure 1). For the centreline and -75m microphones the difference is as much as 5 EPNdB in favour of the Blue Edge™ rotor.

The directivity pattern of BVI propagation for this flight condition needs to be further detailed. Indeed, the noise levels measured on the ground are higher on the retreating blade side for the baseline rotor with its highest values on the centreline and -75m microphones. This implies that the typical advancing parallel interaction (as shown on Figure 1) might be less dominant in this condition than some form of oblique interaction propagating across the aircraft toward the centreline and retreating side. On the other hand the Blue Edge™ noise levels are fairly symmetrical, with a bias toward the advancing blade side for the furthest microphone positions.

In order to better interpret the flight test results, isolated rotor noise predictions were performed using a acoustic solver coupled to a trim and freewake code. This solver, referred to as HMMAP (from the chaining of the various codes: Host-Mesir, Menthe, Arhis, Paris) has been primarly designed at ONERA and is described in detail in Ref. [8]. The HMMAP tool models the trim of the aircraft using the internal Eurocopter flight mechanics code HOST (Ref. [9]), coupled with the freewake code Mesir. The vortex positions and roll-up are then modelled in the Menthe code before the blade-vortex interactions are refined and the resulting pressures are computed by the Arhis code. In the end the noise sources generated by the elastic blade in motion (thickness and loading noise, including BVI) are computed through a Ffwocs-Williams and Hawkings formulation (Ref. [10] and propagated to the ground thanks to the Paris code.

Figure 10 presents the result of this computation for the baseline rotor: the noise footprint generated by the isolated rotor (in a clockwise rotation) at 120m height located over the (0, 0) coordinate point (black circle on the figure) for the 60 knots, -8° glideslope approach. In this representation equivalent to a wind-tunnel mode, the wind comes from the right side of the figure. The same calculation for the Blue Edge™ rotor is presented on Figure 11.

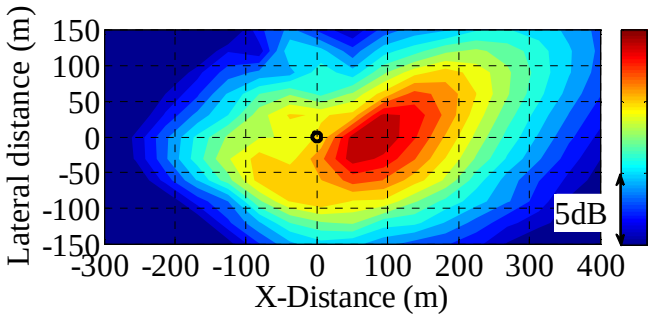

Figure 10 : Noise footprint for isolated reference rotor computed with HMMAP prediction tool.

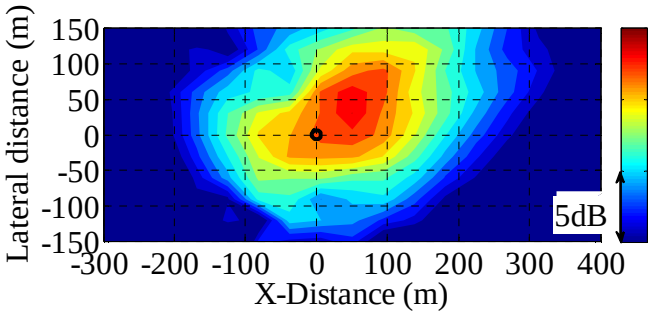

Figure 11 : Noise footprint for isolated Blue Edge™ rotor computed with HMMAP prediction tool.

On Figure 10 the maximum directivity pattern of BVI is clearly centred (maximum noise on the centreline, Y = 0m), but the highest noise regions extend from -50m on the retreating blade side to +50m, on the advancing blade side.

On Figure 11, the BVI region is located on the advancing blade side of the rotor i.e. the positive values of lateral distance (Y-axis).

By comparing the two computations, it can be seen that the isolated rotor prediction results are qualitatively consistent with the measured directivity pattern of Figure 9. In fact, in addition to the strong BVI noise level reduction due to the acoustic phasing effect of the double-swept blade, the previous figures show that the Blue Edge™ blade design drastically changes the baseline rotor directivity pattern, with large noise levels reduction more visible on the centreline and retreating blade side. Indeed, the backward sweep of the Blue Edge™ blades tends to rotate the main directivity pattern toward the advancing side of the rotor. This shift in directivity is beneficial, because it directs the highest noise levels to observers for which the component of the Mach number of the rotating source in their direction is reduced (i.e., the observer is not 'in front' of the moving acoustic source).

The next paragraphs give a detailed analysis of the BVI reduction on the retreating side microphone located 75m from the centreline. On Figure 12 the measured Tone-Corrected Perceived Noise level time-history for the baseline and Blue Edge™ rotors are compared. Both curves are synchronised at the overhead position drawn as a vertical dashed line on the figure.

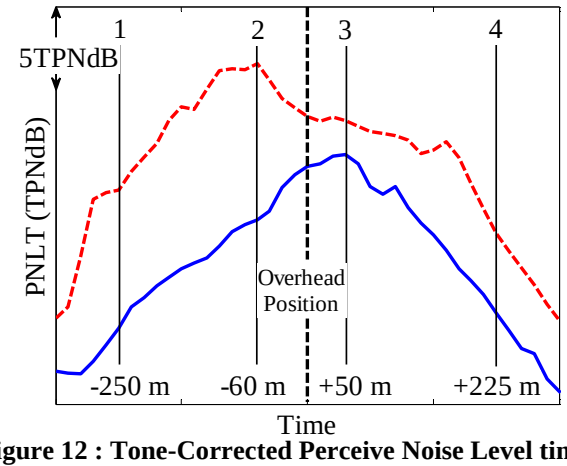

Figure 12 : Tone-Corrected Perceive Noise Level time-history for reference (red dashed curve) and Blue Edge™ (blue solid curve) rotors for a 60 kt, -8° glideslope approach.

Figure 12 shows that the Blue Edge™ rotor reduces the noise on this microphone throughout the aircraft fly-by, and not only on the forward part of the rotor disk as could be expected. The maximum noise reduction is nonetheless observed between 60m to 250m before the aircraft reaches the array, with more than 9 TPNdB reduction when the aircraft is 60m before the array (point 2).

On these approach flights the trajectories for both measurements are similar in position and speed and therefore a direct comparison of time signals can be achieved. On Figure 12 different positions of the rotorcraft at instant of emission are marked from 1 to 4. The noise levels at these emission distances are further detailed in the following acoustic pressure time-history figures.

Figure 13 shows the sound pressure signal as a function of time for the baseline and Blue Edge™ rotors. The time axis for both rotors has been set to two rotor revolutions. These two signals were emitted when the aircraft was positioned 250 m before the centreline microphone and were captured by a microphone located at 75m from the centreline microphone on the retreating blade side of the aircraft. This position matches the instant of the 10 TPNdB below the maximum PNLT for the Blue Edge™ signal.

The two underlying pressure signals are of comparable amplitude. The main difference comes from the series of 3-4 strong BVI peaks that occurs for each passing blade of the baseline rotor. The peaks are also present on the Blue Edge™ signal but the amplitude of the peaks is much less important, and the resulting noise is thus quieter. This is reflected in Figure 12, where a gain of more than 5 TPNdB is demonstrated at -250m.

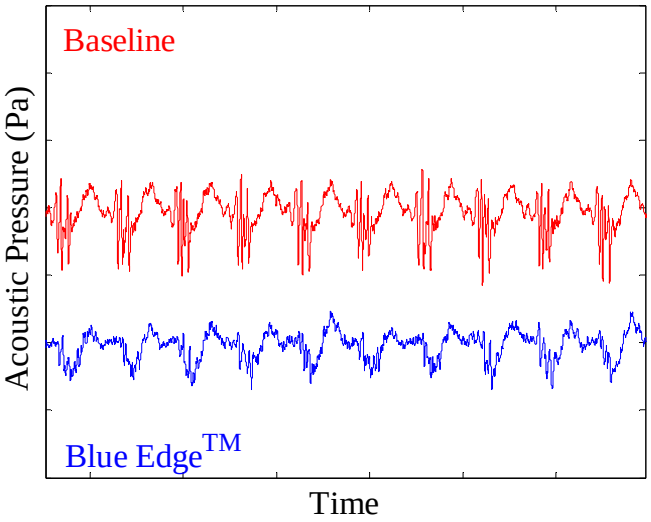

Figure 13 : Acoustic pressure time-history at point 1 (see Figure 12) for reference and Blue Edge™ blades for a 60 kt, -8° glideslope approach (pressure scales are identical).

Figure 14 shows a Fourier transform of the baseline rotor time signal of Figure 13. The acoustic level for each frequency is presented as a function of the main harmonic number. The red triangles localise the pressure level of each harmonic of the main rotor fundamental blade passing frequency. The range on the graph is limited to the 6th to 40th harmonics to focus on BVI content. The same calculation has been made for the Blue Edge™ time-signal on Figure 15. The acoustic pressure range (Y-axis) on both graphs is the same.

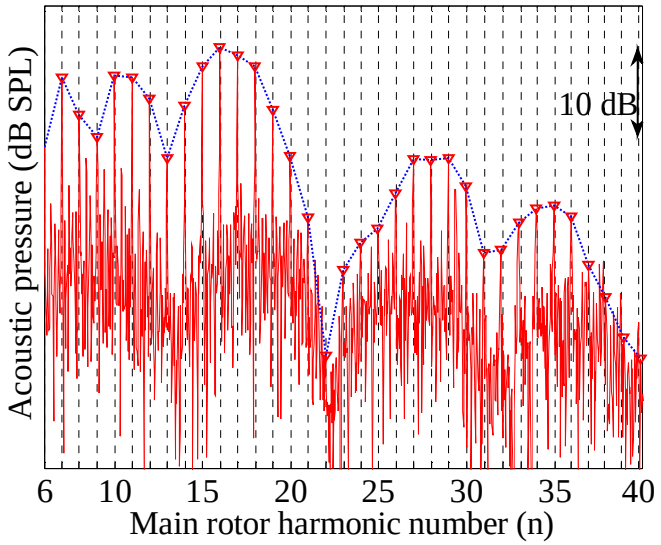

Figure 14 : Sound Pressure level as a function of baseline rotor harmonics at point 1 (Figure 12) for a 60 kt, -8° glideslope approach.

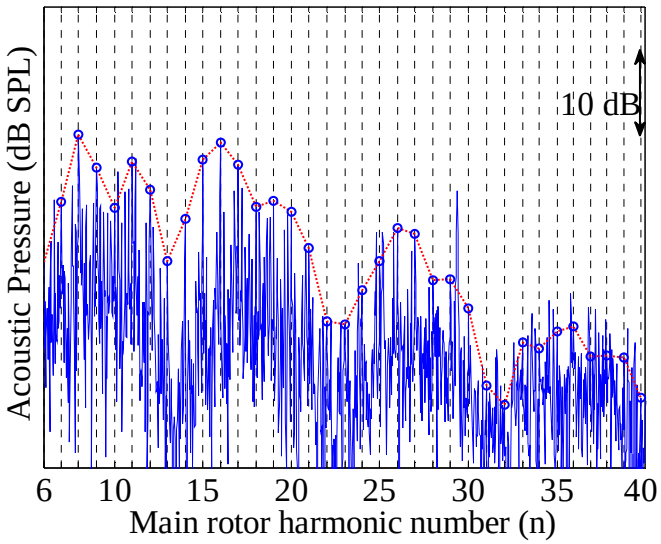

Figure 15 : Sound Pressure level as a function of Blue Edge™ rotor harmonic at point 1 (Figure 13) for a 60 kt, -8° glideslope approach.

On Figure 14 the main rotor harmonics levels have the highest amplitudes of the spectrum and they form a typical envelope dominated by these harmonics. The characteristic regular gaps (for example between harmonics number 22 and 23) are mainly due to ground reflection cancellations, as 1.2m microphones were used during tests.

By studying Figure 15, it is readily seen that from a quantitative point of view the baseline main rotor harmonics are much more present in the spectrum than in the case of Blue Edge™ (much smaller emergence from other sources). This is a direct consequence of the reduction of BVI noise. Note that peak observed before harmonic number 30 is also present on the baseline rotor at a comparable level but in this case it is covered by the main rotor harmonics. This peak is not linked with main rotor acoustic sources. As it is difficult to compare Figure 14 and Figure 15 directly on the same graph, Figure 16 presents a comparative graph using only the main rotor harmonics in the BVI frequency range. As can be seen, all harmonics of the fundamental blade passing frequency of the main rotor are reduced in the case of Blue Edge™, by up to 10-15dB for some harmonics.

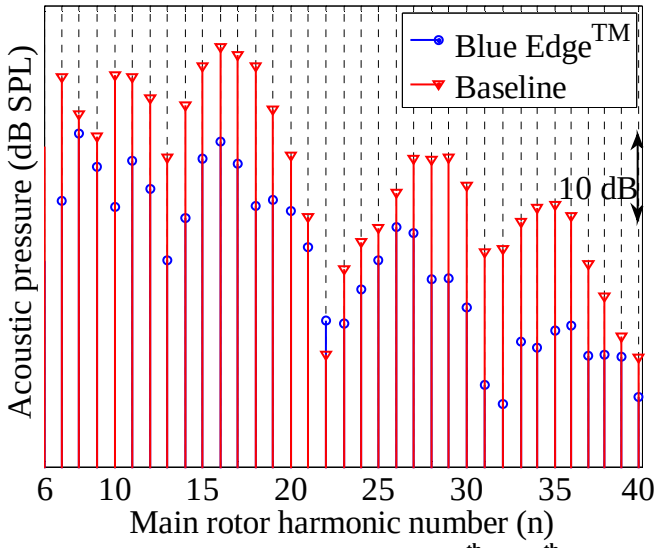

Figure 16 : Sound Pressure level for 6th to 40th rotor harmonics for baseline and Blue Edge rotors at point 1 (Figure 13) for a 60 kt, -8° glideslope approach.

For conciseness, the detailed analysis presented above is not repeated for each point identified on Figure 12, however the evolution of the pressure time-histories are shown for each case.

On Figure 17 the pressure signal extracted at point 2 of Figure 12 are shown, corresponding to the noise emitted when the aircraft is 60m before the centreline microphone; it matches the maximum value of PNLT for the baseline rotor.

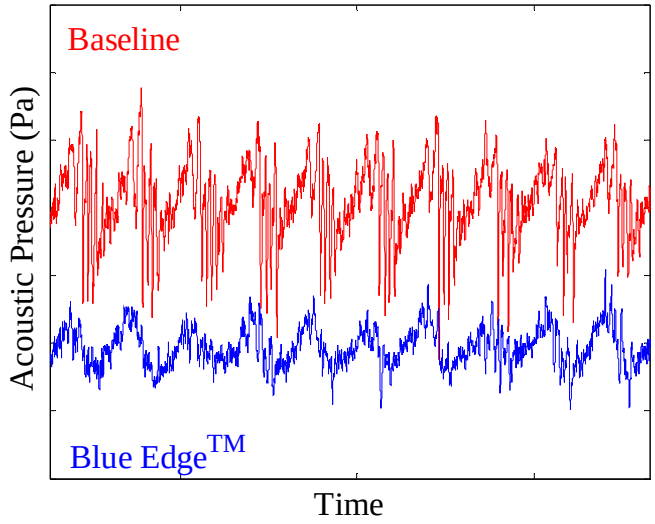

Figure 17 : Acoustic pressure time-history at 2 (60m before overhead position) for reference and Blue Edge™ blades for a 60 kt, -8° glideslope approach.

Once again the difference on the BVI events is obvious: the number and the amplitude of strong peaks have increased for the baseline rotor compared to Figure 13 whereas BVI activity on Blue Edge™ rotor is clearly reduced even if some small BVI peaks can be observed.

Figure 13 and Figure 17 presented impulsive noise signals coming from the aircraft before it reached the microphone. The impulsive acoustic information recorded at these instants results from blade vortex interactions occurring on the advancing blade side and propagating in front of the aircraft. The important noise reductions due to Blue Edge™ are expected in these cases, but what can be surprising on

Figure 12 is that the double-swept rotor also considerably reduces noise levels *after* the aircraft has flown over the microphone array.

Indeed, for point 3 of Figure 12, the aircraft is located 50m after the microphone location and this point represents the instant of maximum PNLT value for the Blue Edge™ rotor. On Figure 18 the pressure time signal of the baseline and Blue Edge™ rotors at point 3 are presented. One can notice that BVI peaks are present in this case, but that their directions have been flipped compared to the BVI peaks of points 1 and 2. Therefore, the noise signal shown in Figure 18 is dominated by BVI occurring on the retreating blade side of the rotor. Again, in this case the Blue Edge™ peak amplitude values are less important, although the same number of BVI peaks is present.

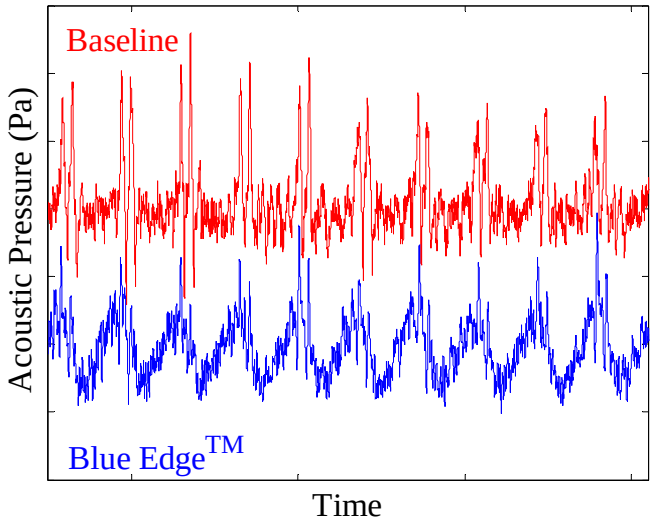

Figure 18 : Acoustic pressure time-history at 3 (50m after overhead position) for reference and Blue Edge™ blades for a 60 kt, -8° glideslope approach.

This reduction of retreating blade BVI noise can be observed in the prediction results shown on Figures 10 and 11, where a BVI hotspot is seen for the baseline rotor at (-50m, -75m).

Finally, the Figure 19 shows the acoustic pressure signals measured at point 4 from Figure 12 (225m after the aircraft crosses the microphone array). This point matches the instant at which the PNLT falls 10dB below the maximum PNLT value for the Blue Edge™ time-history. Again, the figure shows that the baseline rotor exhibits BVI noise generated on the retreating side of the rotor, which is significantly reduced by the double-swept design.

From all these time-signal figures we notice that BVI peaks were strongly present for the baseline rotor and the Blue Edge™ design reduces the number of interactions (less peaks) and also reduces the amplitude of the BVI peaks. The results have shown that for this flight condition the double-swept planform geometry is able to mitigate advancing and retreating side BVI noise. The flight condition shown in this paper was chosen to highlight the most notable differences between the two blades. However, as the near-field results showed, this novel planform geometry successfully reduces BVI in all flight conditions where BVI noise is predominant.

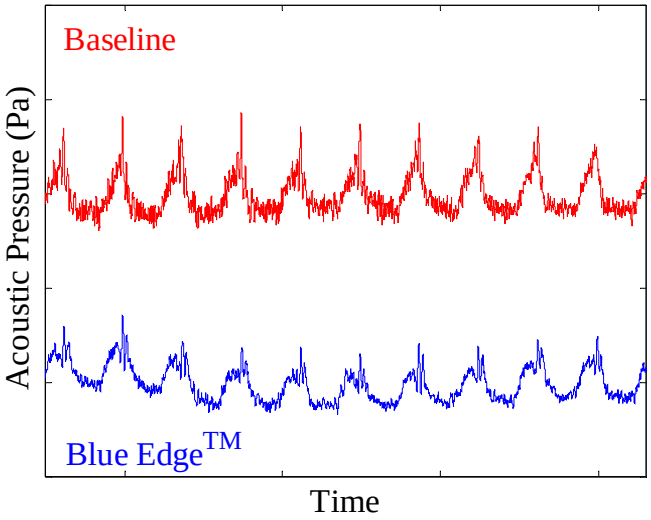

Figure 19 : Acoustic pressure time-history at point 4 (225m after overhead position) for reference and Blue Edge™ blades for a 60 kt, -8° glideslope approach.

Preliminary noise footprint assessment

To assess the environmental impact of the new Blue Edge™ design during typical operations, the acoustical data gathered during the ground measurements are used as an input database to generate noise footprints with the HELENA software (Ref. [11]).

Figure 20 presents the noise footprint obtained from HELENA for the 60 knots, -8° glideslope approach case. Figure 21 is the equivalent noise footprint for the Blue Edge™ rotor. On both graphs the noise level range are the same and the coloured contours are 2 EPNdB apart.

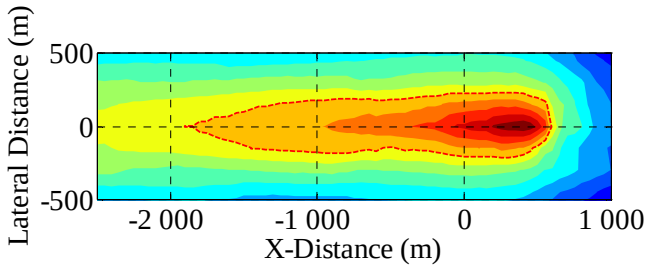

Figure 20 : EPNL noise footprint prediction for baseline rotor in approach phase at 60kt, -8° glideslope (colour contours are 2 EPNdB apart).

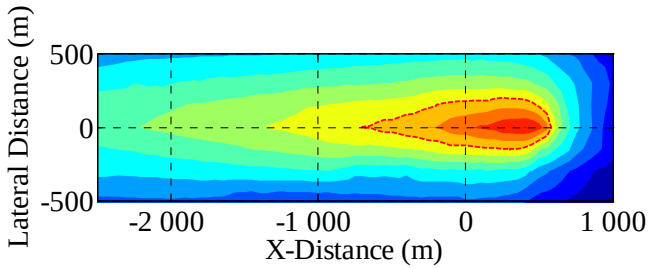

Figure 21 : EPNL noise footprint prediction for Blue Edge™ rotor in approach phase at 60kt, -8° glideslope (colour contours are 2 EPNdB apart).

When comparing these two footprints, it can be observed that the maximum EPNdB noise levels are more important on the reference rotor in the vicinity of the landing point (X=400m, Y=0m). On the advancing blade side (positive lateral distance), the far lateral contours are comparable for

both rotors even if the noise levels are slightly reduced for Blue Edge™ rotor. On the other hand the lateral extent of the contours on the retreating blade side (negative lateral distance) presents noise contour areas which are substantially reduced due to the strong impact of the BVI reduction on Blue Edge™. The area around the centreline exhibits an even more dramatic reduction in contour area.

For example, the area of the contour highlighted in a dashed red line on the previous figures is reduced by more than 60-percent with the Blue Edge™ rotor. In terms of longitudinal extent along the centreline, that particular contour has been reduced by more than 1 km.

CONCLUSION

The acoustic objective of the novel double-swept Blue Edge™ planform was to significantly reduce BVI noise in the approach phase using a passive blade design. This design was based on avoiding the strong acoustic phasing effect that can be encountered in the far-field at certain observer locations with a straight blade. The main conclusions of the acoustic flight test campaigns can be summarised as follows:

- The two comparative flight tests that were performed demonstrated that this concept was indeed successful at drastically reducing the intensity of BVI noise throughout the descending flight envelope of the EC155 five-bladed helicopter compared to the standard straight rotor of that aircraft. No degradation of the noise in climb or forward flight was observed.
- Various metrics were used to analyse the data, and it was shown that the use of the kurtosis allowed a proper identification of BVI noise conditions.
- The main noise reductions were measured close to the centreline, with significant reductions also measured on the retreating side at distances up to 300m from the centreline. This was due both to a reduction of the BVI intensity and to a shift of the directivities caused by the backward sweep.
- The baseline rotor exhibited non-negligible retreating side BVI propagating behind the aircraft, which was significantly reduced by the Blue Edge™ rotor.
- Preliminary noise footprint assessment of a straight-in approach showed that the Blue Edge™ rotor provides a significant reduction of the noise contour area, especially along the flight track.

ACKNOWLEDGMENTS

This study could not have been achieved without the dedication of the Eurocopter flight test team: pilot, flight engineer, and ground team. The authors also wish to acknowledge the valuable work of Sebastien Gradel on the HMMAP tool.

REFERENCES

[1]. Schmitz, F. H. and Sim, B. W., "Radiation and Directionality Characteristics of Helicopter Blade-Vortex Interaction Noise," Journal of the American Helicopter Society, Vol. 48, No. 4, October 2003, pp. 253-269.

[2]. Prieur P. and Splettstoesser W. ERATO – an ONERA-DLR Cooperative Programme on Aeroacoustic Rotor Optimisation. 25th European Rotorcraft Forum, Roma (Italy), September 1999.

[3]. P. Rauch, et all., Blue Edge™: the design, development and testing of a new blade concept, Experiment", Proceedings of the American Helicopter Society 67th Annual Forum, Virginia Beach, VA, May 2011.

[4]. Marze, H., Gervais, M., Martin, P., Dupont, P., Acoustic flight test of the EC130 B4 in the scope of the Friendcopter project, 33rd European Rotorcraft Forum, Russia, Sept. 2007.

[5]. International Civil Aviation Organization, Environmental Protection, Volume 1: Aircraft Noise, Fourth Edition, Amendment 9, International Standards and Recommended Practices, Annex 16 to the Convention on International Civil Aviation, Montreal, Canada, July 2008.

[6]. International Civil Aviation Organization, "Environmental Technical Manual, Volume 1: Procedures for the Noise Certification of Aircraft," First Edition, 2010.

[7]. Abramowitz, M. and Stegun, I. A. (Eds.). Handbook of Mathematical Functions with Formulas, Graphs, and Mathematical Tables, 9th printing. New York: Dover, p. 928, 1972.

[8]. Beaumier P. and Delrieux Y. Description and Validation of the Onera Computational Method for the Prediction of Blade-Vortex Interaction Noise. Aerospace Science and Technology Journal, AST Vol.9 issue 1 (January 2005) 31- 43, Elsevier.

[9]. Benoit, B.; Dequin, A.-M.; Kampa, K.; Gruenhagen, W.; Basset, P.-M. and Gimonet, B., "HOST: A General Helicopter Simulation Tool for Germany and France", 56th American Helicopter Society Annual Forum, Virginia Beach, Virginia, USA, May 2000.

[10]. Ffowcs Williams, J. E., and Hawkings, D. L., "Sound Generated by Turbulence and Surfaces in Arbitrary Motion," Philosophical Transactions of the Royal Society, Vol. A264 (1151), 1969, pp. 321–342.

[11]. M. Gervais, V. Gareton, A. Dummel, R. Heger, Validation of EC130 and EC135 Environmental Impact Assessment Using HELENA, 66th Annual Forum of the American Helicopter Society, Phoenix, AZ, May 2010.